As vacancies, local moments, and Pauli limiting in $LaFeAs_{1-\delta}O_{0.9}F_{0.1}$ superconductors

Vadim Grinenko,[1] Konstantin Kikoin,[1,2] Stefan-Ludwig Drechsler,[1,*] Günter Fuchs,[1] Konstantin Nenkov,[1,3] Sabine Wurmehl,[1] Franziska Hammerath,[1] Guillaume Lang,[1] Hans-Joachim Grafe,[1] Bernhard Holzapfel,[1] Jeroen van den Brink,[1] Bernd Büchner,[1] and Ludwig Schultz[1]

[1]*Leibniz Institute for Solid State and Materials Research IFW–Dresden, P.O. Box 270116, DE-01171 Dresden, Germany*

[2]*School of Physics and Astronomy, Tel-Aviv University, Tel-Aviv IL-69978, Israel*

[3]*International Laboratory of High Magnetic Fields and Low Temperatures, Gajowicka, 95, PL-53-529 Wroclaw, Poland*

(Received 19 May 2011; published 14 October 2011)

We report magnetization measurements of As-deficient $LaO_{0.9}F_{0.1}FeAs_{1-\delta}$ ($\delta \approx 0.06$) samples with improved superconducting properties as compared with As-stoichiometric optimally doped La-1111 samples [i.e., a slightly higher T_c (enhanced by about 2 K) and nearly a twice as large slope of $-dH_{c2}/dT$ at T_c]. In this As-deficient system with almost homogeneously distributed As-vacancies (AV), as suggested by the ^{75}As-nuclear quadrupole resonance measurements, we observe a strong enhancement of the spin susceptibility by a factor of 3–7. This observation is attributed to the presence of an electronically localized state around each AV, carrying a magnetic moment of about 3.2 μ_B per AV or 0.8 μ_B/Fe atom. From theoretical considerations, we find that the formation of a local moment on neighboring iron sites of an AV sets in when the local Coulomb interaction exceeds a critical value of $\sim$1 eV in the dilute limit. Its estimated value amounts to $\sim$2.5 eV and implies an upper bound of $\sim$2 eV for the Coulomb repulsion at Fe sites beyond the first neighbor shell of an AV. Electronic correlations are thus moderate or weak in doped La-1111. The strongly enhanced spin susceptibility is responsible for the Pauli limiting behavior of the superconductivity that we observe in As-deficient $LaO_{0.9}F_{0.1}FeAs_{1-\delta}$. In contrast, no Pauli limiting behavior is found for the optimally doped, As-stoichiometric $LaO_{0.9}F_{0.1}FeAs$ superconductor in accord with its low spin susceptibility.

DOI: 10.1103/PhysRevB.84.134516 PACS number(s): 74.70.Xa, 76.60.−k, 74.25.Ha, 74.25.Op

I. INTRODUCTION

Since the discovery of superconductivity in the Fe pnictides,[1] great efforts have been made to understand the unusual physical properties of these systems. Most of their parent compounds are viewed as itinerant antiferromagnets with a spin density wave (SDW),[2,3] although the strength of correlation effects is still under debate.[4–7] Superconductivity appears by doping, if the antiferromagnetic (AFM) ordering is suppressed. On the other hand, upper critical field measurements at high magnetic fields have shown that many of the iron-based superconductors are limited by the Pauli paramagnetism.[8,9] This limitation should be related to a large paramagnetic spin susceptibility of the conducting electrons in the normal state that mediates the pair breaking of singlet Cooper pairs.[9] So far, to the best of our knowledge, the expected relationship between the Pauli limiting behavior and an enhanced spin susceptibility in the normal state has not yet been confirmed experimentally for the Fe-pnictide superconductors.[10]

A strongly enhanced susceptibility $\chi_s(q = 0)$ would put these systems closer to a ferromagnetic (FM) instability, and it requires a sizable Stoner factor. For example, according to recent investigations,[11] the La-1111 parent compound is already close to such a ferromagnetic instability, which competes with the predominant Fermi-surface nesting driven antiferromagnetic instability. The vicinity of Fe pnictides and related systems to several competing magnetically ordered and superconducting phases seems to be a generic, but not yet well-studied, feature. In this respect, even a relatively small increase of the Stoner factor will result in a sizable enhancement of the paramagnetic susceptibility. It was also pointed out[9] that the local magnetic field can be enhanced by strongly paramagnetic (PM) centers, AFM, or ferromagnetic secondary phases coexisting with the superconducting main phase. For instance, the AFM compound Fe_2As or others may, in high fields, be converted into a highly polarized magnetic state.[9] A general theoretical consideration of possible underlying microscopic mechanisms responsible for the enhanced susceptibility and its relations to the Pauli limiting behavior is still lacking. The La-1111 pnictide is a good model system for such investigations. Recently, Pauli limiting behavior has been found there for optimally doped, polycrystalline $LaO_{0.9}F_{0.1}FeAs_{1-\delta}$ samples with As-vacancies (AV) in the concentration range of $\delta \sim 0.05$–0.1.[8,9,12] In contrast, As-stoichiometric clean $LaO_{0.9}F_{0.1}FeAs$ samples with nearly the same F-doping level do not show any Pauli limiting behavior.[13]

The first indication for an enhanced paramagnetism in As-deficient samples (compared with As-stoichiometric reference samples) came from a strong exponential relaxation of the muon spin polarization observed in μSR measurements.[9] The authors of Refs. 8 and 9 supposed that disorder in the As-deficient sample gives rise to the formation of dilute quasistatic paramagnetic spin clusters of unknown origin. Here, we will demonstrate by a comparative analysis of the static susceptibility data and the ^{75}As-nuclear quadrupole resonance (NQR) spectra together with the nuclear spin-lattice relaxation rate $1/T_1T$ of As-deficient samples that the very vicinity of an AV provides a direct candidate for such paramagnetic centers.

Our paper is organized as follows. In Sec. II, we consider briefly what is known about the concentration of As-vacancies and how the actual concentration can be refined using NQR spectroscopy. Section III deals with the magnetic susceptibility. In Sec. III A, it is explained how the effect of ferromagnetic inclusions is eliminated to get the intrinsic susceptibility analyzed in Sec. III B. Then, we consider theoretical aspects of localized states and local magnetic moments in the frame of Wolff's approach to local moments in a nonmagnetic host.[14] In

Sec. IV, we apply this gained insight to estimate the effective Coulomb repulsion for a localized state derived from the As-vacancy and arrive at an upper bound for the Hubbard U on the Fe sites that bear the superconductivity. In Sec. V, we discuss briefly how the local magnetic moments affect the NMR data. Local-moment-related aspects of Pauli limited superconductivity are considered in Sec. VI. In Sec. VII, we briefly mention a similar situation in Sn-flux-grown Ba-122 superconductors. Finally, we end up with a conclusion containing the gained insight and perspectives for future work.

II. CONCENTRATION OF As-VACANCIES AND THE NQR SPECTRA

Polycrystalline $LaO_{0.9}F_{0.1}FeAs_{1-\delta}$ samples were prepared from pure components using a two-step solid-state reaction method.[15] $LaO_{0.9}F_{0.1}FeAs_{1-\delta}$ samples were obtained by wrapping the samples in a Ta foil during the annealing procedure.[8,9] According to energy dispersive x-ray (EDX) analysis, an As/Fe ratio of about 1.0 was found in the reference sample annealed without a Ta foil and of about 0.9 to 0.95 in the As-deficient samples. At first glance, one might expect an AV gradient within the $LaO_{0.9}F_{0.1}FeAs_{1-\delta}$ samples because the vacancies start to be formed at the surface of the samples. Nevertheless, the sharp superconducting transition width comparable with that of As-stoichiometric reference samples[9] and the surprising temperature dependence of the nuclear spin-lattice relaxation rate $T_1^{-1} \sim T^5$ (the reference samples show $T_1^{-1} \sim T^3$ instead[12,16]) indicate a homogeneous AV distribution within the sample. Additionally, the static susceptibilities $\chi_p(H,T)$ of the As-deficient samples in both the bulk and the surface parts were the same within the error bars of our measurements.

A local characterization was performed using the NQR technique. The ^{75}As NQR spectrum of an As-deficient sample at T =50 K is shown in Fig. 1 together with that of a reference sample.[17] Similar room-temperature data[18] point to a negligible temperature dependence. For As nuclei (spin $I = 3/2$), the measured frequencies obey $\nu_Q \propto Q V_{zz}\sqrt{1+\eta^2/3}$, with Q the electric quadrupole moment, V_{zz} the largest eigenvalue of the electric field gradient tensor, and η the asymmetry of the latter. Whereas the reference samples feature a broad smooth distribution of charge environments, the samples with AVs show several components, as could be expected from varying distances between As nuclei and charged AVs (see also Sec. III C). Since the high-frequency spectral weight is at frequencies rather similar to those of the reference samples, it is likely associated to the As nuclei far away from an AV. The low-frequency spectral weight would accordingly correspond to sites closer to an AV (see Fig. 2). The data were fitted with up to four components (two of them for the low-frequency weight) and assuming that the low-frequency weight corresponds to nearest neighbors (NN) or to both NN and next-nearest neighbors (NNN). In the latter case, two components of equal areas were used, reflecting the assumption that electrostatic repulsion separates the vacancies enough so that each of them features 4 NN and 4 NNN (see Fig. 2). Since the ratio of low- to high-frequency weight is then $4\delta/(1-5\delta)$ (NN) or $8\delta/(1-9\delta)$ (NN + NNN), this leads to $\delta = 0.06(2)$, with the error bar accounting for different fitting procedures. Therefore, the NQR measurements indicate that the AVs are almost homogeneously distributed within the sample volume in the amount as expected from EDX measurements. Future study at other

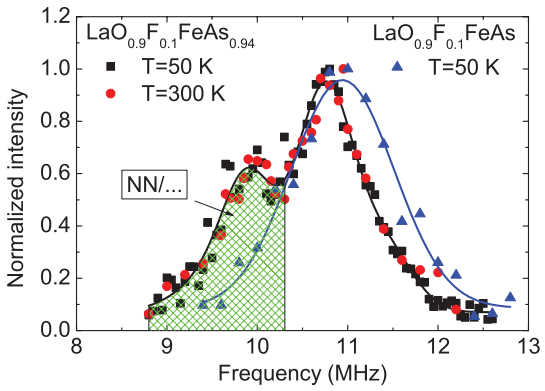

FIG. 1. (Color) ^{75}As NQR spectrum at T = 50 K, together with the spectrum of a reference sample (Ref. 17) and room-temperature measurements (Ref. 18). Black line: a typical fit according to an As-vacancy arrangement shown in Fig. 2. Blue line: broad single-peak fit of the NQR spectrum of a reference sample. NN/. . . and the shaded green area indicate schematically the low-frequency spectral weight below about 10.3 MHz suggested for the NN and NNN shells around an AV as shown in Fig. 2.

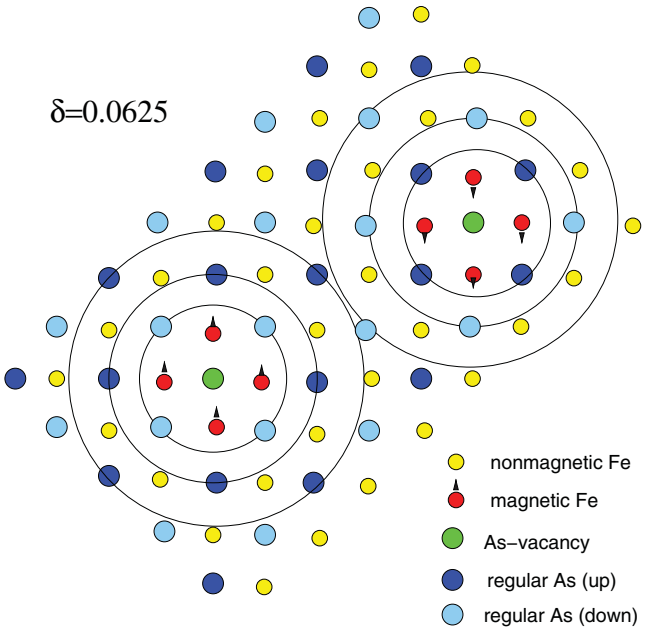

FIG. 2. (Color) Schematic structure of an FeAs block with two neighboring As-vacancies (AV) at a concentration of $\delta = 0.0625$, i.e., in the range suggested by the NQR data shown in Fig. 1 for a typical As-deficient sample. The low-frequency spectral weight below 10.3 MHz is attributed to NN and NNN shells around an As-vacancy, whereas the high-frequency part is attributed to to more distant As sites. Notice the four Fe sites surrounding an AV involved in a local moment. The local magnetic moments are depicted for the simplest case where only the first neighbor shell around an AV is affected (see also text).

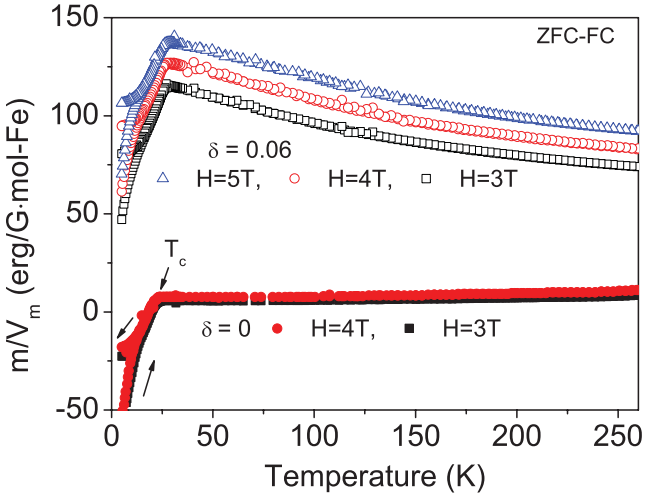

FIG. 3. (Color) Temperature dependence of the magnetization after zero-field cooling at different magnetic fields for $LaO_{0.9}F_{0.1}FeAs_{1-\delta}$.

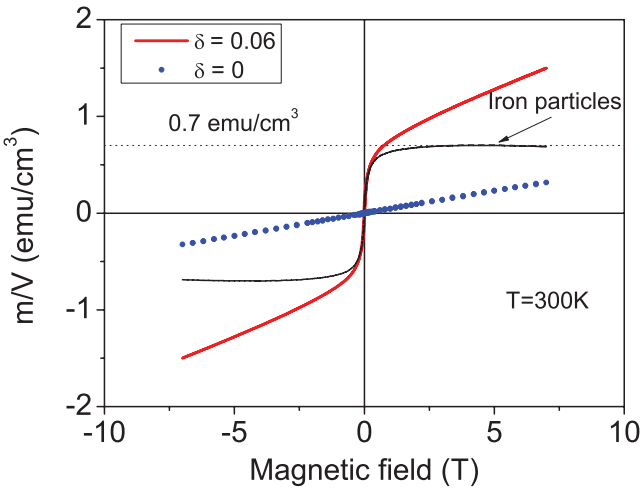

FIG. 4. (Color online) Field dependence of the magnetization of $LaO_{0.9}F_{0.1}FeAs_{1-\delta}$ at 300 K.

compositions will aim at refining this approach, including also the antiferromagnetic parent compound and LiFeAs-derived As-deficient samples without additional disorder caused by F dopants. As a consequence, the widths of the ^{75}As-NQR line in both parent compounds are very small ∼0.1–0.2 MHz,[17,19] in sharp contrast to our F-doped samples.

III. STATIC SUSCEPTIBILITY

In view of the rather specific field and T dependencies of the static magnetization of the As-deficient samples and its large magnitude (see Fig. 3), a more sophisticated analysis of the magnetization is required. The magnetization consists of three main contributions arising (i) from a ferromagnetic (FM) contribution, which we attribute to Fe inclusions (see Sec. III A), (ii) from localized magnetic moments in the very vicinity of a given AV, and (iii) from the T-dependent susceptibility of the Fermi sea of itinerant conduction electrons in which the AV are embedded. The last two contributions are strongly related with each other and can be understood in the framework of Wolff's theoretical approach to impurity effects[14] (see Sec. III C).

A. Iron inclusions

In Fig. 4, the field dependencies of the volume magnetization of two typical $LaO_{0.9}F_{0.1}FeAs$ and $LaO_{0.9}F_{0.1}FeAs_{1-\delta}$ samples are compared at $T = 300$ K. (The magnetization measurements were performed in a Quantum Design DC SQUID.) It is seen that $LaO_{0.9}F_{0.1}FeAs$ has a small paramagnetic magnetization with almost linear field dependence. In sharp contrast, $LaO_{0.9}F_{0.1}FeAs_{1-\delta}$ exhibits a considerably higher magnetization. Its field dependence and the presence of the magnetic hysteresis (see Fig. 5) are an indication of ferromagnetic behavior. At high magnetic fields, the magnetization of a FM material saturates and only a linear paramagnetic contribution remains (see Fig. 4). We suppose that the FM contribution stems from inclusions of pure Fe particles in the As-deficient samples because of (i) a high value of the coercivity field (H_{cor}) and (ii) a rather high Curie temperature of the FM ordering $T_C > 360$ K. These large Fe particles are formed during the heat treatment in contact with a Ta foil since no ferromagnetic inclusions have been observed for the As-stoichiometric reference compound obtained in the same manner despite the final heating in a Ta foil, which produces the AV. In fact, a possible scenario might be as follows: In many Fe pnictides, there is a small amount of $FeAs_2$, FeAs,[20] or other antiferromagnetic inclusions, which become ferromagnetic, and probably are pure Fe inclusions, if a predominant part of As is extracted from them, too. Thus, in the extraction process, As is taken from two kinds of regions: from the pristine regions and from those with inclusions.

The field H_{cor} is related to the particle size of the adopted Fe inclusions. We obtained for the $LaO_{0.9}F_{0.1}FeAs_{1-\delta}$ samples a coercivity field of $H_{cor} \sim 185$ Oe at 300 K (see Fig. 5).

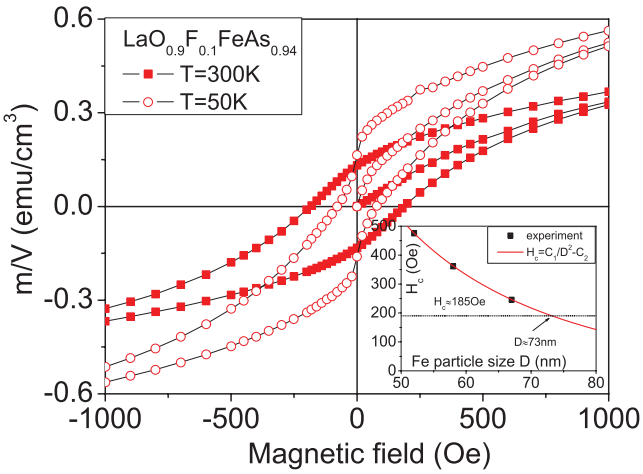

FIG. 5. (Color online) Field dependence of the magnetization of $LaO_{0.9}F_{0.1}FeAs_{0.94}$. Inset: Coercive field H_{cor} of iron particles vs particle size (these experimental data are taken from Ref. 21). The intercept between the fit curve and the horizontal line at 185 Oe gives the minimum size of the iron particles in the $LaO_{0.9}F_{0.1}FeAs_{0.94}$ sample.

Using experimental data for the dependence of H_{cor} on the size of the Fe particles,[21] we estimated for them a size of about 75 nm (see inset in Fig. 5). It is known that the saturation induction of FM materials is independent of the particle size. This allows us to estimate the fraction of the Fe particles in the samples from the magnetization value of $LaO_{0.9}F_{0.1}FeAs_{1-\delta}$. At high magnetic fields, the paramagnetic contribution of the sample can be subtracted from the total magnetization, and the field-independent saturation magnetization is proportional to the Fe fraction in the sample (Fig. 4). At $T = 300$ K, the saturation magnetization of iron $M_{s,Fe} \approx 1.7 \times 10^3$ emu/cm^3 (see Ref. 21), whereas the $LaO_{0.9}F_{0.1}FeAs_{1-\delta}$ samples have at 300 K a saturation magnetization of about $M_{s,def} \approx 0.7$ emu/cm^3. Then, with the unit-cell volume of the As-deficient sample[9] $v_{unit} \approx 0.1415$ nm^3 (i.e., with two Fe atoms per cell) and the sample filling factor of $n_{fill} \approx 0.64$, we estimate for the ratio between Fe atoms in the few FM inclusions and the regular Fe atoms in the As-deficient samples

$$n_{Fe} = \frac{v_{unit} N_a}{2 n_{fill}} \frac{\rho_{Fe} M_{s,def}}{m_{Fe} M_{s,Fe}} \approx 3.9 \times 10^{-3}, \qquad (3.1)$$

where N_a denotes the Avogadro constant, m_{Fe} is the atomic mass of iron, and ρ_{Fe} its density. Thus, we estimate a small atomic fraction of Fe atoms of about 0.4% residing within these ferromagnetic inclusions. Hence, such a small amount of iron has no influence on the estimated effective Fe excess due to the AV, but it nevertheless strongly affects the magnetization curves of the As-deficient samples. Therefore, this inclusion contribution should be subtracted to get the information concerning the static susceptibility.

B. *T* dependence of the paramagnetic susceptibility

As is shown in Fig. 4, the field dependence of the total magnetization becomes linear for magnetic fields exceeding 2 T. Thus, we conclude that the Fe inclusions completely saturate at these fields. To subtract the iron particle's contribution, the T dependence of the magnetic moment of an As-deficient sample after zero-field cooling (ZFC) and at field cooling (FC) was measured at several fields above 2 T (see Fig. 3). For comparison, the T dependence of the magnetic moment of a reference sample $LaO_{0.9}F_{0.1}FeAs$ is also shown at different fields. To get the intrinsic paramagnetic susceptibility of $LaO_{0.9}F_{0.1}FeAs_{1-\delta}$, we subtracted the magnetic moment $m_1(T)$ measured at the field H_1 from the moment $m_2(T)$ measured at the field H_2 and divided this difference by the corresponding field difference:

$$\frac{\Delta m^p}{V_m \Delta H} = \frac{m_2(T) - m_1(T)}{V_m(H_2 - H_1)} = \frac{m_2^p(T) - m_1^p(T)}{V_m(H_2 - H_1)} \approx \chi_p(T). \qquad (3.2)$$

Only paramagnetic moments (m^p) can contribute to $\Delta m = m_2(T) - m_1(T)$ at high fields because the FM contribution is already saturated. At high temperatures, Eq. (3.2) gives the static paramagnetic susceptibility χ_p in [emu/mol-Fe]. Here, V_m is the number of moles per Fe atom. The same procedure was done also for a $LaO_{0.9}F_{0.1}FeAs$ sample taken as a reference system.

The T dependence of the ratios $\Delta m^p / V_m \Delta H$ for both samples above T_c is shown in the inset of Fig. 6. For

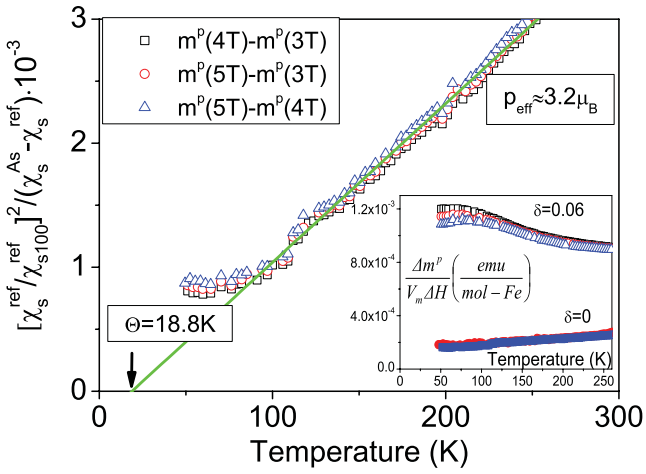

FIG. 6. (Color) The T dependence of the ratio $[\frac{\chi_s^{ref}(T)}{\chi_s^{ref}(T_{ref})}]^2 \cdot \frac{1}{\chi_s^{As}(T) - \chi_s^{ref}(T)}$ for $LaO_{0.9}F_{0.1}FeAs_{1-\delta}$, where χ_s^{ref} and χ_s^{As} are spin susceptibilities of the $LaO_{0.9}F_{0.1}FeAs$ and $LaO_{0.9}F_{0.1}FeAs_{0.94}$. Straight line is a fit by Eq. (3.6). Details of the fitting procedure are described in the text. The ratio $\frac{\Delta m^p}{V_m \Delta H}(\frac{emu}{mol-Fe})$ for two samples defined by Eq. (3.2) is shown in the inset. The closed symbols correspond to $LaO_{0.9}F_{0.1}FeAs$ data for the $m^p(4\,T) - m^p(3\,T)$ and $m^p(2\,T) - m^p(1\,T)$.

$LaO_{0.9}F_{0.1}FeAs$, the susceptibility $\Delta m^p / V_m \Delta H$ linearly increases with the temperature, which is typical for this compound where the AFM spin ordering has been completely suppressed. The absolute value of the susceptibility of the reference samples is similar to that reported by Klingeler *et al.*[22] In contrast, for $LaO_{0.9}F_{0.1}FeAs_{1-\delta}$, the paramagnetic susceptibility is considerably higher and exhibits an unusual T dependence.

First, we suppose that AV can induce local moments. These moments, for example, might occur on a microscopic level just in the vicinity of AV.[9] Possible mechanisms of local moment formation are discussed in Sec. III C. If so, the total number of local magnetic moments in the sample is proportional to the number of AVs δ. These local moments lead to a Curie-Weiss-type contribution at high temperatures[23] (see Figs. 3 and 6):

$$\chi_{Curie}^{As}(T) \approx \frac{C}{T - \Theta} \qquad (3.3)$$

with

$$C = N_a \delta \frac{(p_{eff} \mu_B)^2}{3 k_B}, \qquad (3.4)$$

where Θ is the Curie temperature characterizing the effective strength of magnetic interactions averaged over the whole sample. Its sign reflects the type of this exchange interaction (FM or AFM). In Eq. (3.4), C denotes the Curie constant, $p_{eff} = g[J(J+1)]^{0.5}$, μ_B is the Bohr magneton, g is the Landé factor, J stands for the total electronic angular moment, and k_B is the Boltzmann constant.

Second, these moments are formed in a metallic host with a T-dependent susceptibility. We suppose that this bare host susceptibility of the As-deficient sample is the same as the paramagnetic susceptibility $\chi_p^{ref}(T)$ of the reference

sample. For local moments in a matrix with a T-dependent susceptibility, the experimental data can be analyzed using a method similar to that described in Ref. 23. Therefore, we suppose that the value of the local moment $p_{\rm eff}$ is proportional to the spin susceptibility of the matrix:

$$p_{\rm eff}(T) = \frac{p_{\rm eff}(T_{\rm ref})}{\chi_s^{\rm ref}(T_{\rm ref})}\chi_s^{\rm ref}(T), \tag{3.5}$$

where $T_{\rm ref}$ is some reference temperature. In our case, we have used $T_{\rm ref} = 100$ K as the lowest temperature at which the local paramagnetic susceptibility can be reasonably described by a Curie-type function [see Eq. (3.6) and Fig. 6].

The spin susceptibility $\chi_s^{\rm ref}$ can differ from the paramagnetic susceptibility $\chi_p^{\rm ref}$ due to additional contributions $\chi_{\rm chem}$ from various types of diamagnetism and from the Van Vleck paramagnetism. According to Ref. 11, the estimated (bare) Pauli susceptibility of LaOFeAs from the calculated electronic density of states (DOS) at the Fermi level $N(\varepsilon_F)$ amounts to $\chi_0 \approx 8.5 \times 10^{-5}$ emu/mol-Fe. But, the actual experimental value[22] amounts to $\chi_s = \chi_0(1-I)^{-1} \geqslant 4\chi_0$, where $I = JN(\varepsilon_F)$, i.e., it is significantly enhanced due to the presence of a sizable Stoner factor,[11] where $J \sim 0.7$–0.8 eV (see also Sec. IV). It is known[11,24,25] that $N(\varepsilon_F)$ slightly decreases with F doping. This leads to a decrease of both χ_0 and $N(\varepsilon_F)J$. From the analysis of the experimental data reported in Ref. 22, one can see that at high temperature (above $T_{\rm N}$ of the AFM ordering), the value of the susceptibility reduces only on 15% at the doping level of about ~0.1. Therefore, one expects that $\chi_s^{\rm ref}$ of the reference sample is also strongly enhanced due to a Stoner factor with the corresponding bare spin susceptibility $\chi_0^{\rm ref} \approx 7 \times 10^{-5}$ emu/mol-Fe. From this point of view, we expect that the spin susceptibility $\chi_s^{\rm ref}$ has a dominant contribution to the measured paramagnetic susceptibility $\chi_p^{\rm ref}$ of the reference samples. Hence, we suppose that $\chi_s^{\rm ref} \approx \chi_p^{\rm ref}$.

Finally, according to Ref. 23, the effective susceptibility of a metal with additional extrinsic local moments can be written at high temperatures $T > \Theta$ in the form

$$\chi_s^{\rm As} \approx \chi_s^{\rm ref}(T)\left[1 + \frac{C(T_{\rm ref})}{(T-\Theta)}\frac{\chi_s^{\rm ref}(T)}{\chi_s^{\rm ref^2}(T_{\rm ref})}\right]. \tag{3.6}$$

Our experimental data can be reasonably well described by Eq. (3.6) for $T > 80$ K. The ratio

$$\left[\frac{\chi_s^{\rm ref}(T)}{\chi_s^{\rm ref}(T_{\rm ref})}\right]^2 \frac{1}{\chi_s^{\rm As}(T) - \chi_s^{\rm ref}(T)}$$

is plotted in Fig. 6 where the susceptibility $\chi_s \approx \chi_p$ is defined by Eq. (3.2). The fit by Eq. (3.6) (the straight line) yields $p_{\rm eff} \approx 3.2$, which corresponds to an AV concentration of $\delta \approx 0.06$ and a Curie temperature $\Theta \approx 18.8$ K pointing to dominant FM correlations between the Fe electrons.

C. Formation of magnetic moments

It is well known that nonmagnetic impurities such as Zn induce local moments on neighboring Cu atoms in $YBa_2Cu_3O_{7-\delta}$.[26,27] This effect is not too puzzling because formally isovalent Zn^{2+} impurities substitute for magnetic Cu^{2+} ions in its CuO_2 layers and thus break the Zhang-Rice singlet states. In the case of $LaO_{0.9}F_{0.1}FeAs_{1-\delta}$, the origin of the local moments induced by As-vacancies is less obvious, but eventually the moment formation can be understood if a strong enough d-p hybridization between the As $4p$ and Fe $3d$ orbitals[28] is taken into account. An AV removes the covalent bonds with $3d$ orbitals from four adjacent Fe ions, so the actual defect in the quasi-two-dimensional Fe-As layer is a $[V_{\rm As}Fe_4]$ complex with dangling d-p bonds (cf. Fig. 2). Several effects are related to the formation of this complex. First, the charge transfer from Fe ions to the empty As site results in a local enhancement of the effective charge around Fe ions. The analysis of the reflectivity supports this assumption.[7,9] Second, due to the same charge redistribution, the distance of As atoms from the basal Fe plane in $LaO_{0.9}F_{0.1}FeAs_{1-\delta}$ increases as compared to $LaO_{0.9}F_{0.1}FeAs$.[9] But, the most interesting effect is the possibility of a formation of localized states and related noncompensated magnetic moments around an AV. A more detailed microscopic study will be reported elsewhere.[29] Here, we restrict ourselves mainly to qualitative aspects.

The basic conditions for formation of a nonzero magnetic moment around a nonmagnetic impurity in a paramagnetic metallic host have been formulated in Refs. 14 and 31. In simple terms, a magnetic moment may be formed provided the on-site Coulomb repulsion U of two electrons exceeds some critical value U_c estimated as

$$\frac{U_c}{E_B} \approx \frac{1}{2} + \frac{(\varepsilon_F - E_0)^2}{2\Delta^2}, \tag{3.7}$$

where E_B is the effective bandwidth, ε_F is the Fermi energy, E_0 and Δ are the position and the width of the resonance, respectively, created by the defect in the band. In our case, U is the Coulomb repulsion of two electrons occupying the hybridized d-p orbitals in the $[V_{\rm As}Fe_4]$ complex and the carriers occupy hole pocket around Γ point in the Brillouin zone. The ratio (3.7) may be large enough because each of the 4 Fe ions donates part of its Hubbard repulsion U_0 to the repulsive interaction between the d-p molecular orbitals in the As-vacancy complex. In accordance with this spin-dependent scattering mechanism, a single AV causes the formation of a magnetic moment shared between the adjacent Fe ions. The net magnetic moment associated with a $[V_{\rm As}Fe_4]$ complex defect amounts to about $p_{\rm eff} \approx 3.2$ according to the above estimates. This value corresponds to $\approx 0.8\ \mu_B$/Fe atom, if the magnetic moments occur in the first neighbor shell, only. However, we can not exclude that the second shell is affected as well. In such a case, one is left with two options: parallel or antiparallel spin orientations. Similar results have been obtained in Ref. 32 using local spin-density approximation (LSDA) calculation (i.e., ignoring the local Coulomb repulsion U) for $FeSe_{0.875}/FeTe_{0.875}$ superstructures, i.e., with a twice as large nominal concentration of vacancies and a stronger mutual influence as compared with our title compound and As-vacancies. In the former case, the magnitude of the antiparallel oriented moments at the second neighbor shell was about 1/4–1/3 to that of the first neighbor shell. In other words, then, a relatively large, but far from saturation ($2\ \mu_B$), moment of about 1.067–1.2 μ_B would reside at any Fe site within the first neighbor shell.

A detailed analysis of various spectroscopies may be helpful to elucidate the corresponding local magnetic structure. The relatively large value of the local magnetic moments estimated above should be compared with the regular magnetic moments $\sim 0.4\ \mu_B$ in the magnetically ordered parent compound LaOFeAs.[2] Thus, the magnetic moment induced by an As-vacancy is about two to three times larger than the experimental value observed in the stoichiometric LaOFeAs phase but less than the theoretical value ($\sim 2.3\ \mu_B$) incorrectly predicted by the L(S)DA and other modern band-structure calculations.[2] The resolution of this puzzle is one of the central problems for a future microscopic theory of iron pnictides.

It should be stressed that, in accordance with Wolff's approach,[14] the $[V_{As}Fe_4]$ complexes are isoelectronic defects and, thus, do not affect the carrier concentration. The defect-related structure in the density of states consists of two nearly Lorentzian peaks centered below ε_F (majority spin peak) and above ε_F (minority spin peak). The shift of the Fermi level in comparison with the reference samples seems to be negligible. This is in accord with the observation that the total plasma frequency of an As-deficient sample remains almost unchanged compared to a reference sample.[7] The magnetic moment arises due to this spin-dependent local density of electronic states in the hole band near the Fermi level. Due to the symmetry-related selection rules, the influence of magnetic scattering on the behavior of the electrons in the electronic band is reduced by a factor of $\sim|\mathbf{q}|/|\mathbf{G}|$, where $\mathbf{q}$ is the deviation of the scattering vector from the nesting vector $\mathbf{G}$. The weakness of the umklapp processes makes the single-band Wolff model appropriate for 1111 systems. The vacancy-related defect strongly affects the deep As-4p band, and the side effect of this perturbation is the appearance of a resonance E_0 near the top of the valence As-4p–Fe-3d band around the Γ point. The contribution of 3d states in the electron pocket of the Fermi surface in Eq. (3.7) and its role in formation of local moments around As-vacancies is inessential. Therefore, for the sake of simplicity and clarity, our further analysis will be given within the framework of an effective one-band approach[30] only.

It is important to realize that the strongly anisotropic structure of LaOFeAs prevents clustering of AV since these clusters would induce a large local charge in the Fe plane and strongly increase the potential energy of the lattice. Thus, the lattice anisotropy tends to make the distribution of the AV uniform. This explains why the AVs are relatively homogeneously distributed in our As-deficient samples in spite of the somewhat uncontrollable method of the AV formation. In turn, the charged AVs seem to make the F distribution more homogeneous. This effect can qualitatively explain why As-deficient samples exhibit narrower NQR peaks (Fig. 1) compared to the reference sample. According to Fig. 1, the full width at half maximum (FWHM) of the main NQR peak for the As-deficient sample is only about 0.8 MHz to be compared with the FWHM $\sim$1.3 MHz for the corresponding NQR peak of the reference sample. Moreover, since the size of these magnetic defects is small in comparison with the superconductor coherence length, the former can not essentially reduce the superconducting volume fraction.

Thus, the significant enhancement of the spin susceptibility χ_s^{As} in the As-deficient samples compared to χ_s^{ref} (Fig. 6, inset) may be ascribed to an additional contribution of AV-related magnetic defects to the magnetic response. Then, in accordance with the predictions of the itinerant Wolff model, the susceptibility of a metal containing few impurities with a short-range scattering potential and a strong enough AV-related local Coulomb repulsion factor U_v has the form[31]

$$\chi_s^{\mathrm{As}} = \chi_s^{\mathrm{ref}}\left[1 + \frac{2\delta U_v J \chi_s^{\mathrm{ref}}/R}{1 - U_v J_l \chi_l / R}\right], \tag{3.8}$$

where $\delta \approx 0.06$ is the concentration of the local defects as determined from the EDX and the NQR data mentioned above, $\chi_l = \langle S^+ S^- \rangle_l$ is the local transverse susceptibility of a magnetic defect, $R = 4(g\mu_B/2)^2 N_a/k_B = 1.5$ emu K/mol $\approx 1.29 \times 10^{-4}$ emu eV/mol and $J = 0.7$ eV (is a typical value for 3d electrons in Fe). The operators $S^{\pm}$ given above denote the spin-raising (-lowering) operators, respectively. Since U is supposed to be large enough, the observed enhancement of the spin susceptibility and its δ dependence for our As-deficient samples can be understood at least qualitatively. At high temperatures, Eq. (3.8) yields a Curie-Weiss-type behavior similar to Eq. (3.6). Comparing these equations, we see that the temperature $\Theta \approx 18.8$ K characterizes either some FM correlations between itinerant electrons scattered on the AV or short-range correlations between the localized electrons.

It follows from Eq. (3.8) that the susceptibility χ_s^{As} increases with increasing AV concentration δ. Preliminary data obtained for As-deficient samples with different δ confirm such a behavior. At high AV concentrations, a deviation from the linear dependency of χ_s^{As} on δ is expected. Therefore, further analysis is required to understand the range of applicability of Eq. (3.8).

IV. ESTIMATION OF THE LOCAL COULOMB REPULSION

In general, the parameter $U_v J_l$ and the local susceptibility χ_l are related to each other and should be chosen in a self-consistent way. This is a rather complicated theoretical problem. Its solution would be of considerable interest for future investigations. Here, we will demonstrate that, from the present simple analysis of the experimental data (see Fig. 6), reasonable values of these parameters can be estimated. The relation between the local Coulomb repulsion $U_l = U_v J_l$ for a localized state created by an As-vacancy and the local transverse susceptibility χ_l normalized per χ_s^{ref} is shown in Fig. 7.

The green line is obtained from Eq. (3.7) assuming that the position of the resonance E_0 is very close to ε_F and the effective bandwidth according to band-structure calculations[11,33] amounts to about $E_B \sim 2$ eV. This line denotes the critical strength of $U_l \sim 1$ eV where the formation of a local moment at neighboring iron sites of an AV sets in. In principle, measuring χ_l, the value of U_l could be determined from Eq. (3.8). This would be of considerable interest since, this way, some new insight into the strength of correlation effects in Fe pnictides might be provided. The latter is still under debate and various theoretical estimates scatter in-between 1 and 5 eV,[5–7] although the majority of the community supports a weak or intermediate coupling scenario. (Thereby, we assumed that U_l yields an upper bound for $U_d \approx 2$ eV on iron.) This

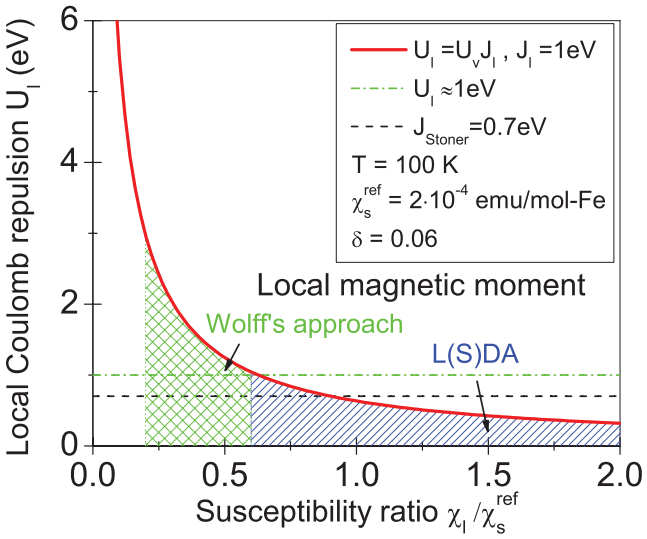

FIG. 7. (Color) The local Coulomb repulsion for a localized state created by an As-vacancy according to Eq. (3.8). The green line denotes the critical strength of U_l where the formation of a local moment at iron sites surrounding an As-vacancy sets in according to Wolff's model. Noteworthy, we admit that local moments can exist also below $U_l = 1$ eV. According to L(S)DA calculations reported in Ref. 32, the formation of the local moments can be expected also in a weakly correlated situation since there is no correlation in the L(S)DA approach.

is in accord with our finding shown in Fig. 6. For example, at $T_{\rm ref} = 100$ K, the susceptibility of the reference sample is $\chi_s^{\rm ref} \approx 2 \times 10^{-4}$ emu/mol-Fe where the ratio between the susceptibilities of the As-deficient and the reference samples amounts to $\chi_s^{\rm As}/\chi_s^{\rm ref} \approx 6$. In fact, in view of the reasonable description achieved by our weak-coupling theory based on the random phase approximation (RPA), we take the susceptibility ratio $\chi_l/\chi_s^{\rm ref}$, say, in-between 0.2 and 0.3, but not below. Then, we estimate for $J_l \approx 1$ eV [see Eq. (4.1)] U_l in between 2.9 and 2 eV, which provides this way an upper bound for U_d. Since U_l should somewhat exceed U_d due to the missing screening from the AV, we adopt also a slightly enlarged J_l as compared with the usual Stoner value of $J \approx 0.7$ eV for Fe (Ref. 11) regarded as a typical value for an Fe site far from the AV in the pnictide superconductor. Then, taking $\chi^{\rm ref} \approx 7 \times 10^{-5}$ emu/mol-Fe (see Sec. III B), we arrive at

$$J_l \approx J \frac{1 - \chi_0^{\rm ref}/\chi_s^{\rm As}}{1 - \chi_0^{\rm ref}/\chi_s^{\rm ref}} \approx 1 \ \text{eV}. \qquad (4.1)$$

With the same screening argument as used above, we then may refine this estimate: $U_d \sim 0.8 U_l \approx 1.6$ to 2.3 eV. This result supports the previous estimates done in Refs. 6 and 7 and is in clear contrast with $U_d > 5$ eV stated recently[5] based on a combined RPA and dynamical mean-field study. In view of the L(S)DA results of Ref. 32 mentioned above, one has to realize that a formation of local magnetic moments might be set in already at much smaller values of U_l or larger ratios of $\chi_l/\chi^{\rm ref}$. This gives further support for a weak-correlation scenario, at least for the occurrence of magnetic moments. To what extent a sufficiently enhanced spin susceptibility can be obtained by that approach, too, remains to be seen.

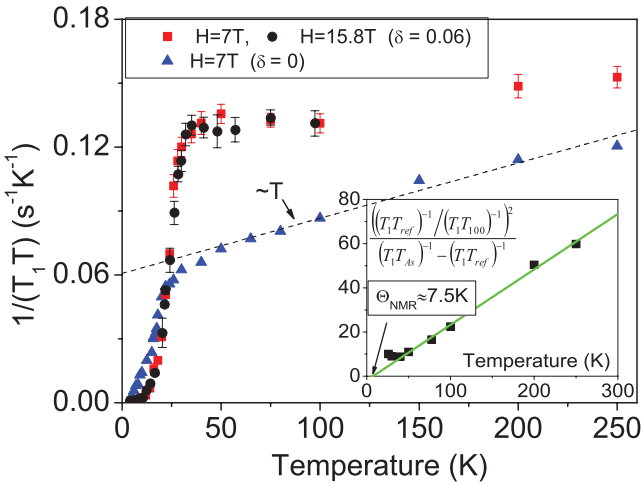

FIG. 8. (Color) ^{75}As spin-lattice relaxation rate $1/T_1T$ versus temperature in $LaO_{0.9}F_{0.1}FeAs_{1-\delta}$. The data are taken from Ref. 12. The steep decrease of both curves reflects the onset of the superconducting transition. The inset shows the T dependence of the ratio $\frac{[(T_1T_{\rm ref})^{-1}/(T_1T_{100})^{-1}]^2}{(T_1T_{\rm As})^{-1}-(T_1T_{\rm ref})^{-1}}$ with $(T_1T_{\rm ref})^{-1}$, $(T_1T_{100})^{-1}$ as the nuclear spin-lattice relaxation rates of $LaO_{0.9}F_{0.1}FeAs$ at arbitrary temperature and at $T_{\rm ref} = 100$ K, respectively, and with $(T_1T_{\rm As})^{-1}$ as the relaxation rate of $LaO_{0.9}F_{0.1}FeAs_{0.94}$. Details of the fitting procedure are described in the text.

V. LOCAL MOMENTS AND NMR DATA REANALYZED

The dynamic spin susceptibility $\chi''(\mathbf{q},\omega)$ of $LaO_{0.9}F_{0.1}FeAs$ and $LaO_{0.9}F_{0.1}FeAs_{1-\delta}$ samples was investigated by ^{75}As NMR spectroscopy.[12,16] The nuclear spin-lattice relaxation rate $1/T_1T$ (where T_1 is the nuclear spin-lattice relaxation time) is directly related to the susceptibility $\chi''(\mathbf{q},\omega)$ summed over all $\mathbf{q}$ in the Brillouin zone.[34] Since the measurement of $1/T_1T$ provides information about the electron-spin susceptibility at all $\mathbf{q}$, we expect that, for As-deficient samples, the presence of enhanced FM correlations characterized by $\mathbf{q} = 0$ should also affect their $1/T_1T$ rate. The temperature dependence of $1/T_1T$ for two typical $LaO_{0.9}F_{0.1}FeAs$ and $LaO_{0.9}F_{0.1}FeAs_{1-\delta}$ samples is compared in Fig. 8 (see also Ref. 12). The inspection in Fig. 8 shows that, above 50 K within the error bars, the $1/T_1T$ of the reference samples can be approximated by a linear T dependence. Since in this temperature range the static susceptibility $\chi_s \propto T$, we can also expect that the $1/T_1T$ of the As-deficient sample can be described by an equation similar to Eq. (3.6) if AVs do not affect essentially the AFM correlations. In this case, the T dependence of the ratio

$$\frac{[(T_1T_{\rm ref})^{-1}/(T_1T_{100})^{-1}]^2}{(T_1T_{\rm As})^{-1} - (T_1T_{\rm ref})^{-1}}$$

should be a straight line, with $(T_1T_{\rm ref})^{-1}$ and $(T_1T_{100})^{-1}$ as the nuclear spin-lattice relaxation rates of the reference samples at arbitrary temperature and at $T_{\rm ref} = 100$ K, respectively, and with $(T_1T_{\rm As})^{-1}$ as the relaxation rate of the As-deficient samples. From the inset of Fig. 8, it is seen that our experimental data can be well described by this empirical fitting procedure.

Therefore, we conclude that the higher relaxation rates of the As-deficient samples can be explained by a contribution related to the local moments formed around AV. Since the contribution of the local moments on the $1/T_1T$ measured on As nuclei is only part of the total field (itinerant electrons apart from AV interact with the As nuclei), the estimated Curie temperature is somewhat lower, $\Theta_{\rm NMR} \approx 7.5$ K, as compared with the usual spin susceptibility derived $\Theta \approx 18.8$ K obtained for the static susceptibility (see Fig. 6), i.e., the hyperfine field for the As nuclei is less affected by the local moments around the AV than the direct magnetic exchange interaction between the electrons.

VI. SUPERCONDUCTING PROPERTIES: ASPECTS OF THE PAULI LIMITING

Up to now, we discussed only high-temperature magnetic properties of As-deficient samples in the metallic normal state phase. But, also the superconductivity of these samples is strongly affected by the induced local magnetic moments. This concerns first of all the T dependence of the upper critical field B_{c2} of the As-deficient samples shown in Fig. 9 (see also Refs. 8 and 9). (Here and below, we ignore possible multiband effects[35] for the sake of simplicity.)

For a polycrystalline sample under consideration, the B_{c2} value refers to those grains that are oriented with their *ab* planes along the applied field. Figure 9 demonstrates that the As-deficient samples exhibit nearly two times higher slopes, $-dB_{c2}/dT$, at T_c compared with the reference samples resulting in a very high orbital upper critical field of $B^*_{c2}(0) =$ 106 T. (The high-field data of the As-stoichiometric optimally doped La-1111 were taken from Ref. 13.) It was supposed previously[8,9] that AVs increase the disorder in FeAs layers and reduce the mean-free path l of the conduction electrons that results in a reduction of the effective coherence length $\xi \sim (\xi_0 l)^{1/2}$. However, the very narrow NQR spectra of the As-deficient samples, as compared with the As-stoichiometric reference samples and the surprisingly stronger T dependence of the nuclear spin-lattice relaxation rate in the superconducting state $T_1^{-1} \sim T^5$ (as compared with $T_1^{-1} \sim T^3$ for the reference sample),[12,16] indicate that actually our As-deficient samples may be even *cleaner* than the reference samples, offering a natural solution of the puzzling problem of unusual or supersmart impurities put forward in Ref. 12. In view of the repulsive interaction between the As-vacancies and an almost homogeneous distribution, the role of remaining, possibly weak, disorder is rather unclear. Therefore, the possible explanation of the reduction of the BCS coherence length $\xi_0 \sim v_F$ for the paired charge carriers in the As-deficient samples may be alternatively explained at least partially by a decrease of the Fermi velocities v_F of conduction electrons due to an additional effective mass enhancement. This may be caused by enhanced magnetic correlations between itinerant electrons in the As-deficient samples. In this respect, further theoretical and experimental work is required to elucidate the origin of such an enhancement. Additionally, as it was pointed out above, the correlated AVs probably lead to a more uniform distribution of the F dopants. This may explain the slightly enhanced $T_c^{\rm As} = 29$ K of the As-deficient samples compared with $T_c = 27.7$ K of the reference samples,[8,9] if the observed FM correlations in As-deficient samples for some reason do not impede the superconductivity.

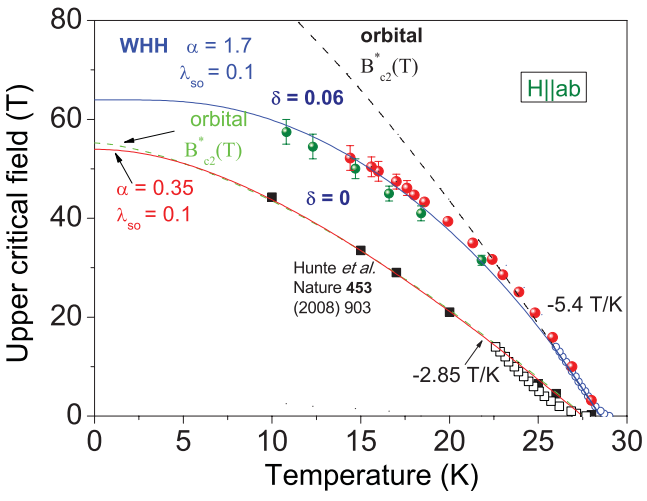

FIG. 9. (Color) Temperature dependence of the upper critical field of $LaO_{0.9}F_{0.1}FeAs_{1-\delta}$. Open circles: dc data, solid circles: pulsed field measurements. Green and red solid circles stand for two different samples from the same batch with the same As-deficiency measured at the Forschungszentrum Dresden and the Institut für Festkörper- und Werkstoffforschung (IFW) Dresden, respectively (Refs. 36 and 37). For comparison, the upper critical field data reported in Ref. 13 are shown (solid squares). Open squares: dc data of the reference sample measured at the IFW Dresden (Ref. 37). Solid lines: fit of the experimental data to the Werthamer-Helfand-Hohenberg (WHH) model. Dashed lines: the orbital upper critical field $B^*_{c2}(T)$.

On the other hand, the resulting critical field at zero temperature $B^{\rm As}_{c2}(0)$ of the As-deficient samples is strongly suppressed by paramagnetic spin effects[8,9] and it may become comparable with the $B^{\rm ref}_{c2}(0)$ of the reference samples in spite of the mentioned larger slope of B_{c2} near T_c and the improved T_c. In general, Pauli limiting behavior is closely related to an enhanced spin susceptibility lowering the free energy in the normal state. In particular, the condensation energy in the superconducting state at zero field and $T = 0$ K is given by the free energy in the normal state at the Pauli limiting field $B_p(0)$:

$$\frac{1}{2}\chi_s^{\rm As} B_p^2(0) = \frac{B_c^2(0)}{8\pi}, \tag{6.1}$$

where $\chi_s^{\rm As}$ is defined in Eq. (3.8). Using Eq. (6.1) and the ratio $\chi_s^{\rm As}/\chi_s^{\rm ref} > 6$ between the spin susceptibilities of the As-deficient and the reference samples, the corresponding ratio $B_p^{\rm As}(0)/B_p^{\rm ref}(0) < 0.4$ between the Pauli limiting fields of both samples can be estimated [where we took into account that, according to our specific-heat measurements, the $B_c(0)$ values of the As-deficient and reference samples are nearly the same]. On the other hand, by fitting upper critical field data for As-deficient samples to the curve predicted by the standard WHH model, the Pauli limiting field $B_p^{\rm As}(0) = 114$ T was estimated[8,9] (see Fig. 9) under the simplifying assumption that the spin-orbital scattering can be neglected ($\lambda_{s0} = 0$). In general, for iron pnictides, the effect of spin-orbit scattering on $B_{c2}(T)$ is expected to be rather weak[9] and we adopt $\lambda_{s0} = 0.1$ as a more realistic value. Then, the resulting Pauli limiting field

is limited by $B_p^{\mathrm{As}}(0) = 88$ T. The same fitting procedure yields $B_p^{\mathrm{ref}}(0) > 200$ T for the reference sample with $\lambda_{s0} = 0.1$. In this case, for the ratio between Pauli limiting fields of two samples, we have $B_p^{\mathrm{As}}(0)/B_p^{\mathrm{ref}}(0) < 0.45$. Therefore, by using the experimentally measured susceptibilities, the observed Pauli limiting behavior can be explained at least qualitatively.

VII. DEFECT AND LOCAL MOMENT ASPECTS IN Ba-122 SYSTEMS GROWN FROM Sn FLUX

Finally, we would like to draw attention, in particular, to the scenario in which Pauli limited superconductivity due to local moments proposed here may be applied also to some K-doped Ba-122 pnictide superconductors. For example, according to Refs. 38 and 39, a similar magnetic behavior as for our As-deficient samples reported here has been observed including Pauli limiting.[40,41] However, at variance with our findings, also a 20% T_c suppression and a broadening of the NMR spectra have been observed pointing to sizable disorder. The peculiar magnetism has been ascribed by the authors to large local moments from a small amount of incorporated Sn occupying As sites,[38,39] this way, being seemingly responsible for a significant paramagnetic pair breaking and the observed T_c suppression. However, in our opinion, a magnetic moment formation around Sn substitutions for As sites seems to be somewhat unlikely. Due to its strong interaction with the Fe-As host, the formation of bound states as a prerequisite for magnetic moments is not expected and instead strong intraband and interband scattering from a nonmagnetic impurity should occur. The latter can readily explain the T_c suppression within any multiband picture, but especially for the $s_{\pm}$-pairing symmetry. Then, the magnetic moments should be attributed to As-vacancies as in this work and/or to Fe residing outside the Fe-As layer. In these single crystals, about 0.05 deficiency of As and about 0.03 excess of Fe have been detected using wavelength dispersive x-ray spectroscopy (WDX).[38] Here, the formation of AV results probably from the Sn flux used in the crystal growth. The former acts as an As getter analogously to the Ta foil in our case and additionally partially replace As atoms. The resulting As deficiency is comparable with that in our As-deficient La-1111 samples. In fact, the mentioned phenomena can be explained semiquantitatively as in this paper.

VIII. CONCLUSIONS

We have measured and analyzed the static susceptibility together with the nuclear spin-lattice relaxation rate $1/T_1T$ of As-deficient samples $LaO_{0.9}F_{0.1}FeAs_{1-\delta}$ ($\delta \approx 0.06$) in comparison with As-stoichiometric reference samples. The concentration of As-vacancies has been first estimated from the EDX analysis and, then, a homogeneous distribution and the amount of vacancies within the samples were confirmed and somewhat refined by NQR measurements. Quite remarkably, the As-deficient samples show a significant enhancement of the spin susceptibility $\chi_s^{\mathrm{As}}/\chi_s^{\mathrm{ref}} \sim 3$–$7$. This enhancement provides experimental evidence that the As-vacancies in the La-1111 compound behave as magnetic defects with a net magnetic moment associated within a $[V_{\mathrm{As}}Fe_4]$ or a $[V_{\mathrm{As}}Fe_8]$ complex defect ($m_{\mathrm{eff}} \approx 3.2\mu_{\mathrm{B}}$). The explanation of this unusual effect is that the As-vacancies induce a local spin polarization of $3d$ electrons near the Fermi energy. The enhanced FM correlations between the conducting electrons are closely related to a high value of the magnetic susceptibility in $LaO_{0.9}F_{0.1}FeAs_{1-\delta}$ via an enhanced Stoner factor. A straightforward consequence of the enhanced spin susceptibility in the As-deficient samples is that their upper critical field is suppressed by spin pair breaking at high external magnetic fields achieved inevitably at low temperature. In contrast, the upper critical field of the reference samples is not affected by the spin pair breaking and it can be described by the orbital $B_{c2}(T)$ contribution down to the lowest temperatures. It would be interesting to elucidate as well the microscopic origin of the Pauli limiting behavior reported also for other Fe pnictide and related selenide and telluride superconductors (see, for example, Refs. 9, 42, and 43). This requires a detailed consideration of the local electronic and magnetic structure of each defect type. Possibly, the local-moment mechanism proposed here can be applied with certain modifications also in those cases, especially in the case of Se- or Te-vacancies.[43] Investigations of the spin susceptibility and NQR measurements of these compounds are a necessary prerequisite, thus being of considerable interest. In general, a better understanding of the new and complex physics induced by various real defects present in many samples can also provide valuable insight into the superconducting mechanism itself, into the role of correlation effects under debate, and into the complex interplay with several competing magnetic and superconducting phases.

ACKNOWLEDGMENTS

Discussions with K. Koepernik, R. Klingeler, D. Efremov, A. Yaresko, M. Kiselev, I. Eremin, M. Korshunov, M. Kulic, V.A. Gasparov, J. Málek, S. Haindl, A. Köhler and G. Behr are gratefully acknowledged. We thank P. Canfield for critical discussion at an earlier stage of this study. J.v.d.B., S.L.D., and K.K. (Grant No. BR4064/3-1), H.J.G. (Grant No. GR3330/2), as well as S.W. and B.B. (Grant No. BE1749/13) would like to thank the DFG Priority Programme SPP1458 "High Temperature Superconductivity in Iron Pnictides" for financial support. V.G. would like to thank the Marie Curie Research Training Network (RTN) NESPA, MRTN-CT-2006-035619, under the EU 6th Framework Programme for financial support. S.W. acknowledges also support by the DFG under the Emmy-Noether program (Grant No. WU595/3-1).

*s. l.drechsler@ifw-dresden.de

[1] Y. Kamihara, T. Watanabe, M. Hirano, and H. Hosono, J. Am. Chem. Soc. **130**, 3296 (2008).

[2] C. de la Cruz, Q. Huang, J. W. Lynn, J. Li, W. Ratcliff II, J. L. Zarestky, H. A. Mook, G. F. Chen, J. L. Luo, N. L. Wang, and Pengcheng Dai, Nature (London) **453**, 899 (2008).

[3] M. Rotter, M. Tegel, D. Johrendt, I. Schellenberg, W. Hermes, and R. Pöttgen, Phys. Rev. B **78**, 020503 (2008).

[4] L. Hozoi and P. Fulde, Phys. Rev. Lett. **102**, 136405 (2009).

[5] A. Kutepov, K. Haule, S. Y. Savrasov, and G. Kotliar, Phys. Rev. B **82**, 045105 (2010).

[6]W. L. Yang, A. P. Sorini, C.-C. Chen, B. Moritz, W.-S. Lee, F. Vernay, P. Olalde-Velasco, J. D. Denlinger, B. Delley, J.-H. Chu, J. G. Analytis, I. R. Fisher, Z. A. Ren, J. Yang, W. Lu, Z. X. Zhao, J. van den Brink, Z. Hussain, Z.-X. Shen, and T. P. Devereaux, Phys. Rev. B **80**, 014508 (2009).

[7]S.-L. Drechsler, H. Rosner, M. Grobosch, G. Behr, F. Roth, G. Fuchs, K. Koepernik, R. Schuster, J. Malek, S. Elgazzar, M. Rotter, D. Johrendt, H.-H. Klauss, B. Büchner, and M. Knupfer, e-print arXiv:0904.0827.

[8]G. Fuchs, S.-L. Drechsler, N. Kozlova, G. Behr, A. Köhler, J. Werner, K. Nenkov, R. Klingeler, J. Hamann-Borrero, C. Hess, A. Kondrat, M. Grobosch, A. Narduzzo, M. Knupfer, J. Freudenberger, B. Büchner, and L. Schultz, Phys. Rev. Lett. **101**, 237003 (2008).

[9]G. Fuchs, S.-L. Drechsler, N. Kozlova, M. Bartkowiak, J. E. Hamann-Borrero, G. Behr, K. Nenkov, H.-H. Klauss, H. Maeter, A. Amato, H. Luetkens, A. Kwadrin, R. Khasanov, J. Freudenberger, A. Köhler, M. Knupfer, E. Arushanov, H. Rosner, B. Büchner, and L. Schultz, New J. Phys. **11**, 075007 (2009).

[10]Recently, we have learned that similar enhanced magnetism as reported here caused by local magnetic moments of "impurities" as well as Pauli limiting behavior have been observed for some Ba-122 superconductors (Refs. 40 and 41). But, the important interrelation between the two phenomena and physical consequences have not been mentioned (see also Sec. VII).

[11]D. J. Singh and M.-H. Du, Phys. Rev. Lett. **100**, 237003 (2008).

[12]F. Hammerath, S.-L. Drechsler, H.-J. Grafe, G. Lang, G. Fuchs, G. Behr, I. Eremin, M. M. Korshunov, and B. Büchner, Phys. Rev. B **81**, 140504(R) (2010).

[13]F. Hunte, J. Jaroszynski, A. Gurevich, D. C. Larbalestier, R. Jin, A. S. Sefat, M. A. McGuire, B. C. Sales, D. K. Christen, and D. Mandrus, Nature (London) **453**, 903 (2008).

[14]P. A. Wolff, Phys. Rev. **124**, 1030 (1961).

[15]A. Kondrat, J. E. Hamann-Borrero, N. Leps, M. Kosmala, O. Schumann, A. Köhler, J.Werner, G. Behr, M. Braden, R. Klingeler, B. Büchner, and C. Hess, Eur. Phys. J. B **70**, 461 (2009).

[16]H.-J. Grafe, D. Paar, G. Lang, N. J. Curro, G. Behr, J. Werner, J. Hamann-Borrero, C. Hess, N. Leps, R. Klingeler, and B. Büchner, Phys. Rev. Lett. **101**, 047003 (2008).

[17]G. Lang, H.-J. Grafe, D. Paar, F. Hammerath, K. Manthey, G. Behr, J. Werner, and B. Büchner, Phys. Rev. Lett. **104**, 097001 (2010).

[18]G. Lang, H.-J. Grafe, F. Hammerath, K. Manthey, D. Paar, G. Behr, J. Werner, J. Hamann-Borrero, and B. Büchner, Phys. C (Amsterdam) **470**, 5454 (2010).

[19]I. Morozov, A. Boltalin, O. Volkova, A. Vasiliev, O. Kataeva, U. Stockert, M. Abdel-Hafiez, D. Bomber, A. Bachmann, L. Harnagea, M. Fuchs, H.-J. Grafe, G. Behr, R. Klingeler, S. Borysenko, C. Hess, S. Wurmehl, and B. Büchner, Cryst. Growth Des. **10**, 4428 (2010).

[20]P. J. Baker, H. J. Lewtas, S. J. Blundell, T. Lancaster, F. L. Pratt, D. R. Parker, M. J. Pitcher, and S. J. Clarke, Phys. Rev. B **78**, 212501 (2008).

[21]R. K. Dumas, C.-P. Li, I. V. Roshchin, I. K. Schuller, and K. Liu, Phys. Rev. B **75**, 134405 (2007).

[22]R. Klingeler, N. Leps, I. Hellmann, A. Popa, U. Stockert, C. Hess, V. Kataev, H.-J. Grafe, F. Hammerath, G. Lang, S. Wurmehl, G. Behr, L. Harnagea, S. Singh, and B. Büchner, Phys Rev. B **81**, 024506 (2010).

[23]A. M. Clogston, B. T. Matthias, M. Peter, H. J. Williams, E. Corenzwit, and R. C. Sherwood, Phys. Rev. **125**, 541 (1962).

[24]P. Larson and S. Satpathy, Phys. Rev. B **79**, 054502 (2009).

[25]L. Boeri, O. V. Dolgov, and A. A. Golubov, Phys. Rev. Lett. **101**, 026403 (2008).

[26]A. V. Mahajan, H. Alloul, G. Collin, and J. F. Marucco, Phys. Rev. Lett. **72**, 3100 (1994).

[27]H. Alloul, J. Bobroff, M. Gabay, and P. J. Hirschfeld, Rev. Mod. Phys. **81**, 45 (2009).

[28]D. R. Garcia, C. Jozwiak, C. G. Hwang, A. Fedorov, S. M. Hanrahan, S. D. Wilson, C. R. Rotundu, B. K. Freelon, R. J. Birgeneau, E. Bourret-Courchesne, and A. Lanzara, Phys Rev. B **78**, 245119 (2008).

[29]K. Kikoin, S.-L. Drechsler, J. Málek, and J. van den Brink (unpublished).

[30]Accounting of the electron band contribution in a two-band generalization of Eq. (3.8) in the form that the spin susceptibility of a reference sample $\chi_s^{\rm ref} = \chi_s^h + \chi_s^{el}$ consists of a hole $\chi_s^h \geqslant 3/4$ and an electron $\chi_s^{el} \leqslant 1/4$ contribution results in minor changes [about several percent in the estimated local Coulomb repulsion U_l (see Sec. IV)]. Thereby, we adopted a slightly less but still dominant contribution from the hole bands to the total DOS of a reference sample with an F-doping level of $\sim$0.1 as compared with that of the calculated one for the undoped parent compound in the paramagnetic state (Ref. 11).

[31]D. L. Mills and P. Lederer, Phys. Rev. **160**, 590 (1967).

[32]K.-W. Lee, V. Pardo, and W. E. Pickett, Phys. Rev. B **78**, 174502 (2008).

[33]V. Vildosola, L. Pourovskii, R. Arita, S. Biermann, and A. Georges, Phys. Rev. B **78**, 064518 (2008).

[34]C. H. Pennington and V. A. Stenger, Rev. Mod. Phys. **68**, 855 (1996).

[35]A. Gurevich, Phys. Rev. B **82**, 184504 (2010).

[36]G. Fuchs, S.-L. Drechsler, N. Kozlova, J. Freudenberger, M. Bartkowiak, J. Wosnitza, G. Behr, K. Nenkov, B. Büchner, and L. Schultz, J. Low Temp. Phys. **159**, 164 (2010).

[37]G. Fuchs, S.-L. Drechsler, N. Kozlova , V. Grinenko, J. Freudenberger, M. Bartkowiak, G. Behr, C. Hess, R. Klingeler, A. Köhler, K. Nenkov, H.-H. Klauss, B. Büchner, and L. Schultz, J. Phys.: Conf. Ser. **234**, 012013 (2010).

[38]N. Ni, S. L. Bud'ko, A. Kreyssig, S. Nandi, G. E. Rustan, A. I. Goldman, S. Gupta, J. D. Corbett, A. Kracher, and P. C. Canfield, Phys. Rev. B **78**, 014507 (2008).

[39]Sutirtha Mukhopadhyay, Sangwon Oh, A. M. Mounce, Moohee Lee, W. P. Halperin, N. Ni, S. L. Bud'ko, P. C. Canfield, A. P. Reyes, and P. L. Kuhns, New J. Phys. **11**, 055002 (2009).

[40]M. M. Altarawneh, K. Collar, C. H. Mielke, N. Ni, S. L. Bud'ko, and P. C. Canfield, Phys. Rev. B **78**, 220505 (2008).

[41]V. A. Gasparov, L. Drigo, A. Audouard, D. L. Sun, C. T. Lin, S. L. Bud'ko, P. C. Canfield, F. Wolff-Fabris, and J. Wosnitza, e-print arXiv:1104.5619.

[42]G. Fuchs, S.-L. Drechsler, N. Kozlova, M. Bartkowiak, G. Behr, K. Nenkov, H.-H. Klauss, J. Freudenberger, M. Knupfer, F. Hammerath, G. Lang, H.-J. Grafe, B. Büchner, and L. Schultz, Phys. C (Amsterdam) **470S1**, S288 (2010). See Fig. 3 and references therein.

[43]S. Khim, J. W. Kim, E. S. Choi, Y. Bang, M. Nohara, H. Takagi, and K. H. Kim, Phys. Rev. B **81**, 184511 (2010).